Identification of old drugs as potential inhibitors of HIV-1 integrase - Human LEDGF/p75 interaction via molecular docking

ARTICLE *in* JOURNAL OF MOLECULAR MODELING · JUNE 2012

Impact Factor: 1.74 · DOI: 10.1007/s00894-012-1494-0 · Source: PubMed

8 AUTHORS, INCLUDING:

Xianqiang Sun
Washington University in St. Louis
20 PUBLICATIONS **91** CITATIONS
SEE PROFILE

Guixia Liu
East China University of Science and Techn…
63 PUBLICATIONS **877** CITATIONS
SEE PROFILE

Xu Shen
Shanghai Institute of Materia Medica, Shan…
245 PUBLICATIONS **4,222** CITATIONS
SEE PROFILE

Yun Tang
East China University of Science and Techn…
149 PUBLICATIONS **2,167** CITATIONS
SEE PROFILE

J Mol Model (2012) 18:4995–5003
DOI 10.1007/s00894-012-1494-0

ORIGINAL PAPER

Identification of old drugs as potential inhibitors of HIV-1 integrase – human LEDGF/p75 interaction via molecular docking

Guoping Hu · Xi Li · Xianqiang Sun · Weiqiang Lu · Guixia Liu · Jin Huang · Xu Shen · Yun Tang

Received: 8 April 2012 / Accepted: 5 June 2012 / Published online: 26 June 2012

Abstract Integration of viral-DNA into host chromosome mediated by the viral protein HIV-1 integrase (IN) is an essential step in the HIV-1 life cycle. In this process, human protein Lens epithelium-derived growth factor (LEDGF/p75) is discovered to function as a cellular co-factor for integration. LEDGF/p75-HIV-1 IN interaction represents an attractive target for anti-HIV therapy. In this study, approved drugs were investigated for the finding of potential inhibitors on this target. Via molecular docking against the LEDGF/p75-binding pocket of HIV-1 IN, 26 old drugs were selected from the DrugBank and purchased for bioassays. Among them, eight, namely Atorvastatin, Bumetanide, Candesartan, Carbidopa, Diclofenac, Diflunisal, Eprosartan, and Sulindac, were identified as potential inhibitors of LEDGF/p75- HIV-1 IN interaction, whose IC_{50} values ranged from 6.5 μM to 36.8 μM. In addition, Atorvastatin was previously reported to block HIV-1 replication and may have an important implication for the treatment of AIDS. Our results suggested a mechanism of action for the anti-HIV effects of Atorvastatin. This work provides a new example of inhibitors targeting protein-protein interaction and confirmed that old drugs were valuable sources for antiviral drug discovery.

Keywords Drug repositioning · HIV-1 Integrase · Human LEDGF/p75 protein · Molecular docking · Protein-protein interaction

Guoping Hu and Xi Li contributed equally to this work.

Electronic supplementary material The online version of this article (doi:10.1007/s00894-012-1494-0) contains supplementary material, which is available to authorized users.

G. Hu · X. Li · X. Sun · W. Lu · G. Liu · J. Huang (✉) · Y. Tang (✉)
Shanghai Key Laboratory of New Drug Design, School of Pharmacy, East China University of Science and Technology, Shanghai 200237, China
e-mail: huangjin@ecust.edu.cn
e-mail: ytang234@ecust.edu.cn

X. Shen
State Key Laboratory of Drug Research, Shanghai Institute of Materia Medica, Chinese Academy of Sciences, Shanghai 201203, China

Introduction

Human immunodeficiency virus type 1 (HIV-1) is a big threat to human health. Currently there are more than 30 drugs in the market for the treatment of HIV-1 infection. However, the virus could develop rapid resistance to those drugs due to high mutation rate. In order to overcome the resistance, new drugs with novel mechanisms of action should be developed.

HIV-1 integrase (IN) is a vital enzyme which catalyzes the insertion of proviral DNA into host cell genome. This is an essential step in retroviral replication [1]. HIV-1 IN comprises three structurally and functionally distinct domains: the amino terminal domain (residues 1-50), the catalytic core domain (residues 51-212) and the carboxyl terminal domain (residues 213-288). With these three domains, IN performs the integration process which consists of two subsequent steps: 3'-processing and strand transfer. Raltegravir which is the first US FDA-approved drug targeting HIV-1 IN on the strand transferring step would incur Raltegravir-resistant HIV shortly after administration [2].

To overcome HIV-1 resistance, medications with novel mechanisms of action should be developed. It was found that human cellular cofactors play key roles in HIV-1 IN performing function [3]. Among them, lens epithelial-cell-derived growth factor (LEDGF, also referred to as p75) was identified in complex with HIV-1 IN and plays an essential

role in the distribution of IN in the nucleus, which is the key procedure for viral replication [4]. Experiments confirmed that p75 bound to HIV-1 IN via a small, approximate 80-residue IN-binding domain (IBD) within its C-terminal region. IBD of p75 was mapped to residues 347–429 and interacted specifically with the IN core domain [5]. p75-mediated chromatin tethering depended on specific interactions between the p75 IBD and the IN core domain. Therefore, it was speculated that disturbing or blocking p75-IN interaction would prevent the replication of the virus [6–8].

Recently, the complex structure of p75 with HIV-1 IN (PDB code: 2B4J) was determined by X-ray crystallography [9], which provides the basis of structure-based drug design. However, targeting protein-protein interaction was thought to be a tough job because of the comparatively large and flat interface [10]. Fortunately, in the case of p75-IN interaction, the IBD of p75 inserted into a relatively small and deep cleft at the interface of IN catalytic core domain (CCD) dimmer, which therefore brought a good chance for rational design of inhibitors targeting p75-IN interaction.

In a previous study, we reported that compound **D77** (see Fig. 1) could specifically bind at the p75-IN interaction interface [11], and it was the first confirmed inhibitor to interrupt p75-IN interaction. The second inhibitor was CHIBA-3003 (Fig. 1), whose IC_{50} value was 35 μM by AlphaScreen assay [12]. Recently, compound **3** and compound **6** (Fig. 1) were proven to block the interaction between p75 and IN by complex crystal structures (PDB code: 3LPT and 3LPU) [13]. Their IC_{50} values were 12 μM and 1 μM, respectively. Notably, compound **6** could retain full potency against all five Raltegravir-resistant strains, which indicated its diverse mode of action. More recently, a series of compounds were developed based on the core structure of CHIBA-3003. Among them, CHIBA-3003_5h showed the most potency with IC_{50} value at 3.5 μM in AlphaScreen assay (Fig. 1) [14]. De Luca et al. [15] published a detailed review on inhibitors of this target recently.

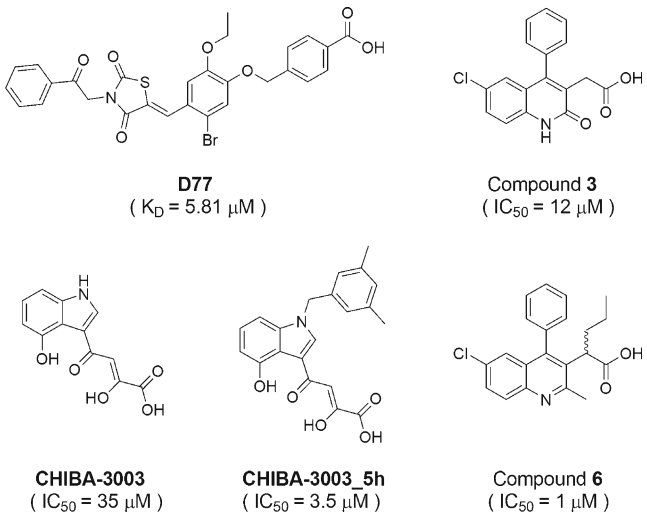

Fig. 1 Representative structures of p75-IN interaction inhibitors

Since there are more than one thousand FDA approved drugs available in the DrugBank (http://www.drugbank.ca/), whose structural types are diverse and pharmacological features are well known, the study of these drugs might provide new examples for the treatment of HIV-1 positive AIDS in a short period of time. A few old drugs were finally confirmed to show potent inhibitory activities against the p75-IN interaction. This study confirmed that old drugs are valuable sources for antiviral drug discovery.

Materials and methods

Protein preparation

The docking were performed using IN structure alone retrieved from X-ray crystallographic of the dimeric catalytic core domain of HIV-1 IN complexed with LEDGF/p75 IBD deposited in the RCSB Protein Data Bank (entry code: 2B4J). In this structure, there were two gaps in chain A, and one gap in chain B. Prime 2.1 [16] was used to rebuild the gaps based on one crystal structure of IN (PDB code: 1BL3). The fixed protein was submitted to Schrodinger's Protein Preparation Wizard. Bond orders and charges were thus assigned, and the orientation of hydroxy groups, amide groups of Asn and Gln, and the charge state of His residues were optimized. Energy minimization was carried out using MacroModel 9.7 [17] with default setting. Coordinates for the p75 tri-peptide Ile365-Asp366-Asn367 were taken directly from the C chain of the PDB 2B4J crystal structure and used as a control to generate the docking grid file. This model was named as 2B4J_IN.

Model validation

To evaluate the performance of 2B4J_IN, virtual screening capability of this model was compared to that of two crystal structures (PDB code: 3LPT and 3LPU). The database used for subsequent simulated virtual screening test was composed of 11 reported inhibitors (IC_{50}<20 μM) (listed in Table S1, supporting information) and 1000 decoys. The decoys were selected based on the protocols of Discovery studio 2.5 [18]. Firstly, commercial compound were retrieved from database-Specs (http://www.specs.net/) and filtered by rule of 5. Secondly, with the "find diverse molecules" protocol, 10,000 diverse compounds were chosen from the 70,624 molecules. Finally, with the "find similar molecules by fingerprint" protocol, 1000 similar compounds were obtained from these 10,000 diverse molecules using the 11 known p75-IN interaction inhibitors as references. During this process, similarity calculation was

first performed between the 10,000 diverse molecules and the 11 actives based on FCFP_4 fingerprint, and then the top 1000 molecules sorted by the Tanimoto similarity index values were collected as the decoy set. These three consecutive steps not only ensured the structural diversity of selected decoys but also kept them localized near the chemical space of the active molecules. This process has been confirmed to be reliable by a previous study of our group [19, 20]. Subsequently, the database was screened on the three models.

In this study, the "receiver operating characteristic" (ROC) enrichment (ROCE) was adopted to evaluate the VS performance [21], defined as the ratio of active rate to the decoy rate at a given stage where a particular percentage of the decoys are observed [22]. The relationship between the ROC value and ROCE for a predefined false positive fraction is given by the following:

$$\text{ROC enrichment}@\text{X\%} = \frac{\frac{N^{X\%}_{\text{actives selected}}}{N_{\text{total actives}}}}{\frac{N^{X\%}_{\text{decoys selected}}}{N_{\text{total decoys}}}} = \frac{\frac{TP}{TP+FN}}{\frac{FP}{TN+FP}} = \frac{\text{sensitivity}}{1-\text{specificity}} = \frac{\text{y value ROC point}}{\text{x value ROC point}}. \quad (1)$$

To show the capability of the active enrichment during the early stage of VS, ROCEs with decoy rates of 0.5 %, 1.0 %, 2.0 % and 5.0 % were calculated, as suggested by Jain and Nicholls [23]. ROCE values above 1.0 indicate that the enrichments are better than random values at different decoy stages. ROC enrichments for three models were calculated and compared. The ROC enrichment values indicated clearly that 2B4J_IN could yield the highest early enrichment, as illustrated in Fig. 2. Therefore, 2B4J_IN was adopted as our screening model.

Database preparation

The DrugBank 2.0 contained 1467 drugs. Before molecular docking, two filtering steps were adopted: molecules with molecular weight lower than 75 or larger than 600 were removed at first; then only those containing at least one carboxyl group were chosen to proceed. It is interesting to notice that most of the reported inhibitors of p75-IN interaction contained a carboxyl group which could form hydrogen-bonds with key residues in IN hydrophilic subpocket and therefore, was used as a filter. Thus the 229 drugs obtained were docked against 2B4J_IN. Before docking, these compounds were prepared with Ligprep 2.3 [24]. During this process, OPLS_2005 force field was chosen and the possible ionization states at the pH range of 5.0-9.0 were generated. Thus the carboxylate group of each compound is ionized (without proton) because its pKa lies outside the pH range.

Molecular docking experiments

Docking studies were performed using Glide 5.5 [25] standard precision (SP) [26]. Glide SP provided flexible docking for the ligands. Glide uses a hierarchical series of filters to search for possible ligand locations in the active-site region of the receptor. All default settings were used for docking. After the Glide SP docking, the precise ligand-receptor binding free energy for each ligand was calculated using MM-GBSA provided by the "Prime MM-GBSA" module [16]. The "Take complexes from a Maestro Pose Viewer file" selection was chosen and only the top ranked molecules (glide gscore<-5.0) provided by Glide SP, were submitted for running the MM-GBSA calculation. All protein atoms were frozen, and only the ligand structures were relaxed during the MM-GBSA calculation. Simultaneously, the ligand strain energies were calculated [27]. The "Prime DG bind" energy of the Prime MM-GBSA with ligand strain was chosen for the rescoring function. Drugs with "Prime MM-GBSA DG bind" score < -30 kcal mol^{-1} were stored for visual analysis to check the docking poses and interactions between ligands and receptor. Finally, 26 drugs were selected and purchased for AlphaScreen assays.

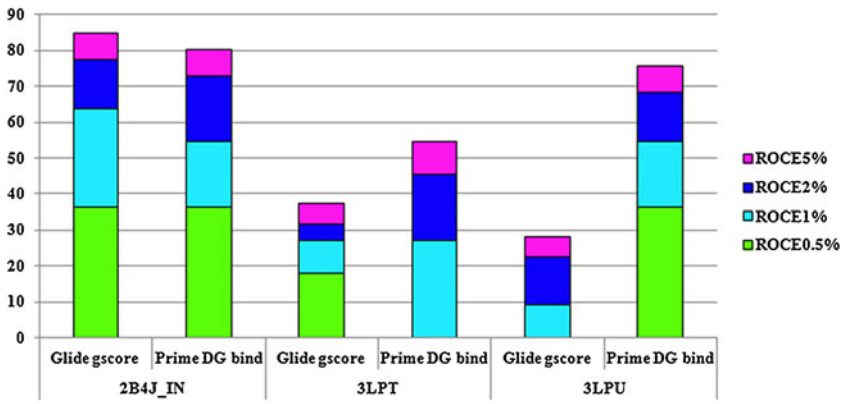

Fig. 2 ROC enrichment of "Glide gscore" and "Prime MM-GBSA DG bind" for three screening models

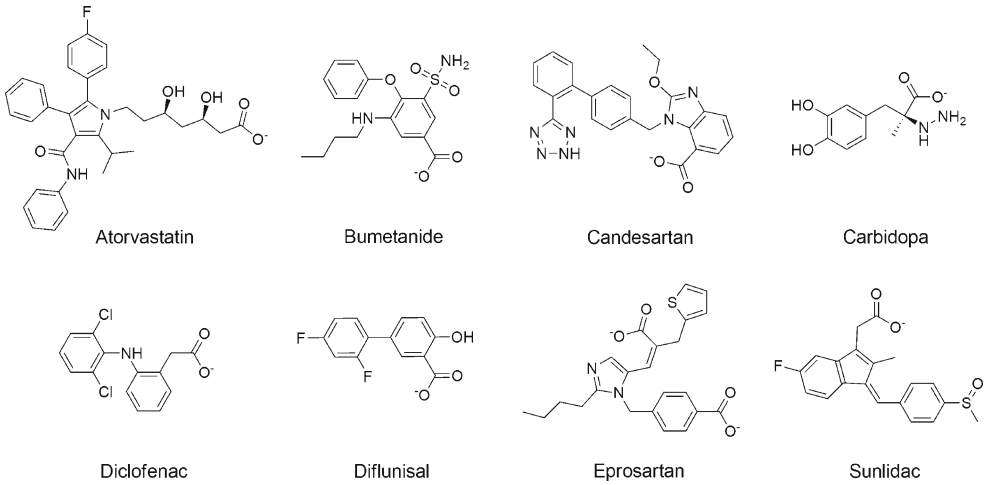

Fig. 3 Chemical structures and inhibitory activities of eight old drugs on p75-IN interaction

Bioassay method (AlphaScreen technology)

The HIV-1 IN CCD was expressed and purified as described in reference [28]. The IBD of p75 (residues 347-442) containing GST tag was prepared as described previously [11]. The p75-IN AlphaScreen assay was developed as described previously [29]. Reactions were performed in a 25 µl final volume in 384-well ProxiPlates (PerkinElmer) in assay buffer (25 mM HEPES, pH 7.3, 150 mM NaCl, 2 mM $MgCl_2$, 1 mM DTT and 0.1 % BSA). The His_6-tagged HIV IN_CCD was added to a final concentration of 40 nM and incubated with compound varying concentration from 0.1 µM to 100 µM at room temperature for 30 min. Afterward, the remaining components containing GST-tagged p75 IBD (final 40 nM), Nickel Chelate Acceptor Beads (final 8 μg/mL) and Glutathione Donor Beads (final 8 μg/mL) were added to the well. Proteins and beads were incubated at room temperature for 2 h. The incubation was performed in the dark to avoid direct light exposure. The plates were measured in the EnVision multilabel plate reader (PekinElmer) with the final emission of 520-620 nm.

Results and discussion

Bioassay results

Compound **3** was reported as a potent inhibitor of p75-IN interaction with an IC_{50} value at 12.2 μM [13]. In this study, compound **3** was purchased and used as a positive control. Among the 26 purchased compounds, eight showed inhibitory activities (IC_{50} values ranging from 6.5 μM to 36.8 μM, Table 1). Particularly, Carbidopa and Atorvastatin were quite potent with IC_{50} values at 6.54 μM and 8.90 μM, respectively. The IC_{50} value of compound **3** was 11.65 μM, which was quite close to the reported value as mentioned above. This result also confirmed the accuracy and reliability of our bioassays. The chemical structures of the eight old drugs were shown in Fig. 3.

Table 1 Inhibitory activities of 26 selected drugs as well as compound 3

Drugs Name	DrugBank ID	LEDGF/p75-IN interaction	
		Inhibition[a] (%)	IC_{50} (μM)[b]
Argatroban	DB00278	7.29	ND
Atorvastatin	DB01076	51.85	8.90±1.11
Bezafibrate	DB01393	28.45	ND
Bumetanide	DB00887	32.15	13.53±1.87
Candesartan	DB00796	42.26	11.36±1.29
Carbidopa	DB00190	62.02	6.54±0.94
Diclofenac	DB00586	47.07	21.95±7.38
Diflunisal	DB00861	42.76	17.71±4.17
Enoxacin	DB00467	0	ND
Eprosartan	DB00876	43.67	36.85±1.36
Fenoprofen	DB00573	2.61	ND
Flurbiprofen	DB00712	3.37	ND
Fluvastatin	DB01095	15.45	ND
Ibuprofen	DB01050	22.03	ND
Indomethacin	DB00328	30.42	ND
Ketoprofen	DB01009	11.06	ND
Lomefloxacin	DB00978	2.23	ND
Montelukast	DB00471	16.03	ND
Nalidixic Acid	DB00779	22.34	ND
Naproxen	DB00788	25.4	ND
Niflumic Acid	DB04552	17.16	ND
Olopatadine	DB00768	10.76	ND
Sulindac	DB00605	33.75	13.85±2.60
Tazobactam	DB01606	0	ND
Telmisartan	DB00966	3.03	ND
Tolmetin	DB00500	11.09	ND
Compound 3		45.13	11.65±1.12

[a] Compounds at 10 μM concentration. [b] IC_{50} data are presented as mean ± SD. ND, not determined

Analysis of p75-IN interface

IN was recognized by p75 through two key features, as illustrated in Fig. 4. One is the specific backbone conformation of residues 168-171 which can form a hydrogen-bond network with IBD, the other is a hydrophobic patch accommodating the side chains of p75 residues Ile365, Phe406 and Val408 [9]. Namely, there are two subpockets for ligand binding, one is hydrophilic, and the other is hydrophobic. Residue Asp366 of p75 formed a bidentate hydrogen bond with the backbone amides of IN residues Glu170 and His171 in chain A. Residue Ile365 projected into a hydrophobic pocket formed by residues Leu102, Ala128, Ala129, Trp132 of IN chain B and Thr174, Met178 of chain A. Through molecular dynamics simulation of p75 and IN, Zhao et al. [30] found that three stable hydrogen bonds at the interface of IN and p75 were closely related to residues Gln168, Glu170 and Thr174. Residue Asp366 formed stable hydrogen bonds with Glu170 and Thr174, as well as an intermittent hydrogen bond with His171. The contribution of residues Thr125 and Trp131 in chain B were significant to the binding affinity of IN and p75. Site mutagenesis studies highlighted the role of Gln168 and Trp131 [31].

Our previous work reported the discovery of **D77** targeting the interface of p75 and HIV-1 IN [11]. Via site-directed mutagenesis, four residues, namely Gln95, Thr125 and Trp131 in chain B and Thr174 in chain A were identified to be crucial for the binding of **D77**.

Many strong protein-ligand interactions are characterized by extensive lipophilic contacts. An extension of the lipophilic contact surface between protein and ligand often leads to an improvement in the binding affinity. This means that the search for unoccupied lipophilic pockets in the protein should be one of the first steps to design and optimizing novel ligands. Using GRID molecular interaction fields, De Luca et al. [14] explored a new binding pocket region for small molecular inhibitors. This area corresponded to the hydrophobic region located near Trp131 in B chain. Site mutagenesis studies also highlighted the role of Trp131 [31]. Taking together, key residues for inhibitor recognition are Gln168, Glu170, His171, and Thr174 in chain A and Glu95, Thr125, Trp131 in chain B.

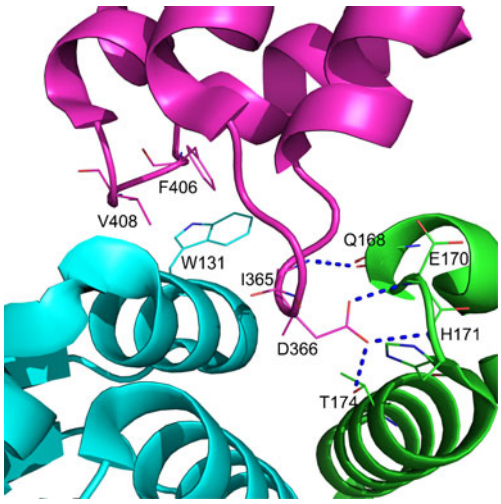

Fig. 4 Key contacts at the IBD-CCD interface. IBD is colored in magenta. Chain A is colored in green, chain B is colored in cyan. Selected residues are shown as lines. Blue dash lines represent hydrogen bonding

Binding mode analysis of old drugs

The binding modes of eight old drugs at the interface of IN were illustrated in Fig. 5. The detailed binding mode of each drug was analyzed as follows.

Atorvastatin consists of multiple aromatic rings and a polar fatty acid side chain containing two hydroxyl groups. Figure 5A shows a possible binding mode of Atorvastatin and suggests following interactions: a) the carboxylate group forms hydrogen bonds with the backbone of Glu170, side chain of His171, Thr174 in chain A and Gln95 in chain B; b) one of the hydroxyl groups forms a hydrogen bond with Thr125 of chain B; c) the aniline part shows hydrophobic contacts for the crucial Trp131 of chain B as suggested by GRID studies. The distance between them is about 3.8 Å; therefore, they might form a π-π stacking interaction.

Bumetanide contains two polar functional groups. One is carboxylate group and the other is sulfamide group. Figure 5B shows predicted binding mode of Bumetanide, which exhibits the following interactions: a) the carboxylate group forms hydrogen bonds with the backbone of Glu170, side chain of His171, Thr174 in chain A and Gln95 in chain B; b) the sulfamide group forms a hydrogen bond with the backbone carbonyl group of IN residue Gln168 of chain A; c) the butyl group projects into the hydrophobic pocket.

Candesartan has two polar functional groups. One is the carboxylate group and the other one is the tetrazole moiety which can be considered as an isosteric replacement of the carboxylate group. Figure 5C shows the predicted binding mode of Candesartan, exhibiting the following interactions: a) the carboxylate group forms hydrogen bonds with the backbone of Glu170, side chain of His171, Thr174 in chain A and Gln95 in chain B; b) the fused benzene ring of the imidazole scaffold projects into the hydrophobic pocket; c) the biphenyl group connecting the tetrazole moiety jumps out of binding pocket and might form extended hydrophobic interactions.

Carbidopa has four polor functional groups including one carboxylate group, one hydrazine group and two phenolic hydroxyl groups. Figure 5D shows predicted binding mode of Carbidopa and four key interactions are identified: a) the carboxylate group forms hydrogen bonds with the backbone

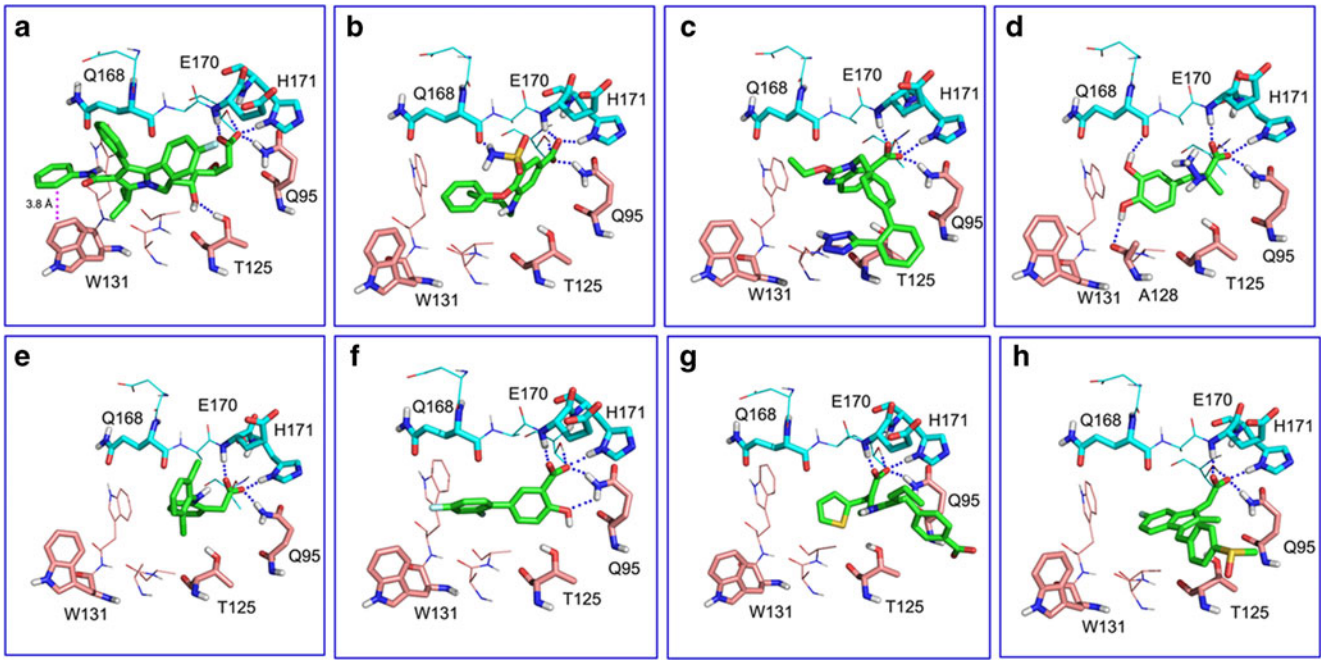

Fig. 5 Binding modes of **a** Atorvastatin, **b** Bumetanide, **c** Candesartan, **d** Carbidopa, **e** Diclofenac, **f** Diflunisal, **g** Eprosartan, and **h** Sulindac at the p75-binding pocket of IN (ligand colored in green). Dash lines represent non-bonded interactions between the ligand and receptor: blue, H-bonding; pink, π-π interaction

of Glu170, side chain of His171, Thr174 in chain A and Gln95 in chain B; b) one of phenolic hydroxyl group forms a hydrogen bond with the backbone carbonyl group of Gln168 in chain A; c) another phenolic hydroxyl group forms a hydrogen bond with the backbone carbonyl group of Ala128 of chain B; d) the hydrophobic pocket is occupied by the benzene ring.

Diclofenac contains a phenyl acetic acid substructure. Figure 5E shows a plausible binding mode of Diclofenac, exhibiting the following interactions: a) the carboxylate group forms hydrogen bonds with the backbone of Glu170, side chain of His171, Thr174 in chain A and Gln95 in chain B; b) the benzene ring connecting acetic acid lies in the hydrophobic pocket.

Diflunisal contains a salicylic substructure. Figure 5F shows the predicted binding mode of Diflunisal, exhibiting the following interactions: a) the carboxylate group forms hydrogen bonds with the backbone of Glu170, side chain of His171, Thr174 in chain A and Gln95 in chain B; b) the phenolic hydroxyl group creates an additional hydrogen bond with Gln95 of chain B; c) the biphenyl group occupies the hydrophobic pocket formed by residues of chain B.

Eprosartan has two carboxylate groups. Figure 5G shows the plausible binding mode of Eprosartan, exhibiting the following interactions: a) the carboxylate group forms hydrogen bonds with the backbone of Glu170, side chain of His171, Thr174 in chain A and Gln95 in chain B; b) the thiophene group projects into the hydrophobic pocket; c) the benzoic acid group binds to the main-chain of Gly94 and Gln95 of chain B.

Sulindac contains an aryl acetic acid substructure. Figure 5H shows the predicted binding mode of Sulindac, exhibiting the following interactions: a) the carboxylate group forms hydrogen bonds with the backbone of Glu170, side chain of His171, Thr174 in chain A and Gln95 in chain B; b) the indene ring system occupies the hydrophobic pocket formed by IN chain B residues.

The binding modes of eight old drugs revealed that all the carboxyl groups of these compounds fitted well in the IN hydrophilic pocket and formed hydrogen bonds with Glu170, His171, Thr174 of chain A and Glu95 of chain B. In addition to the carboxyl groups, Bumetanide formed a hydrogen bond with Gln168 of chain A; Diflunisal formed an additional hydrogen bond with Gln95 of chain B. It is noted that Carbidopa formed two additional hydrogen bonds with Gln168 of chain A and Ala128 of chain B and exhibited the most potent inhibitory activity. Atorvastatin, the second potent compound, formed two additional interactions with Thr125 and Trp131. These results suggested that in order to improve activity, inhibitors should contain some additional functional groups to interact with Gln168, Thr125, Ala128, or Trp131 in addition to carboxyl groups. Candesartan, Diclofenac, Eprosartan, and Sulindac also exhibited inhibitory activities without forming additional hydrogen bonding with Gln168, Thr125, and Ala128 or π-π stacking interaction with Trp131. Their activities might be due to some nonpolar interactions. Although Eprosartan formed additional hydrogen bonds

with Gly94 and Gln95 of chain B, the hydrophobic pocket was less occupied. This might be one reason for its lower activity.

Superimposition of eight active drugs and the crystal structure of p75 bound to the pocket of HIV-1 IN indicate that all of them bind to p75 binding pocket of HIV-1 IN as illustrated in Fig. 6. The observations in this study could provide a reasonable explanation for active drugs exhibiting their inhibitory activities. These active drugs can serve as lead compounds to further explore the anti-HIV mechanism by disturbing the interaction between p75 and IN. Three drugs with molecular weight lower than 300 could be further optimized to improve their activities.

A potent inhibitor targeting the interaction between p75 and IN is CHIBA-3003_5h reported by De Luca et al. [14] with IC_{50} value 3.5 μM. CHIBA-3003_5h represents a good example forming hydrophobic interaction with the hydrophobic region near Trp131. Based on our model, a superimposed Atorvastatin with CHIBA-3003_5h indicated clearly that they had a quite similar binding mode, as shown in Figs. 7a and b. Both of them had a comparatively long polar anchor. In addition to the carboxyl group, both CHIBA-3003_5h and Atorvastatin formed a hydrogen bond with Thr125. They all extended their hydrophobic part into the hydrophobic region around Trp131. It was m-xylene part in CHIBA-3003_5h and aniline group in Atorvastatin that form hydrophobic interaction with Trp131. Notably, the distance between phenyl of aniline and aromatic ring of Trp131 is about 3.8 Å, they might form an "edge to face" π-π interaction. The main difference between two binding modes was that the hydrophobic pocket was well occupied by CHIBA-3003_5h but less occupied by Atorvastatin.

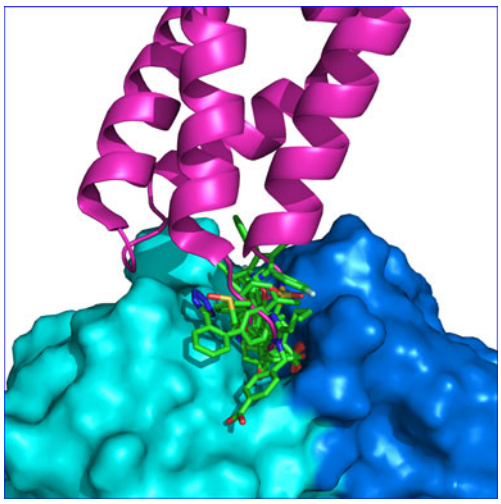

Fig. 6 Superimposition of eight active drugs and the crystal structure of p75 bound to the pocket of HIV-1 IN (PDB code: 2B4J). Molecular surfaces are shown for IN (**a** chain in blue, **b** chain in cyan). IBD of p75 is shown in magenta

Anti-HIV mechanism of Atorvastatin

Statin compounds represent a well-established class of drugs which can be used to decrease serum cholesterol levels and are widely prescribed for the treatment of hypercholesterolemia. Atorvastatin is a potent inhibitor of HMG-CoA reductase, clinically used to decrease the level of blood lipid. Because the serum lipoprotein concentrations of AIDS patients are often increased after taking protease inhibitors, statins were therefore often used to treat the high cholesterol of AIDS patients [32]. Interestingly, previous studies suggested that if the amount of cholesterol in infected cells was reduced, multiplication of HIV can also be reduced [33].

To explain this phenomenon, two mechanisms were proposed. One mechanism proposed was that statins target Rho GTPase and affected the virus entry or budding [33]. Previous data suggested that the anti-HIV effect of statins might be due to the inhibition of isoprenoid biosynthesis; consequently, Rho GTPase could not be prenylated at their C-terminus to fulfill its function. This would inhibit the

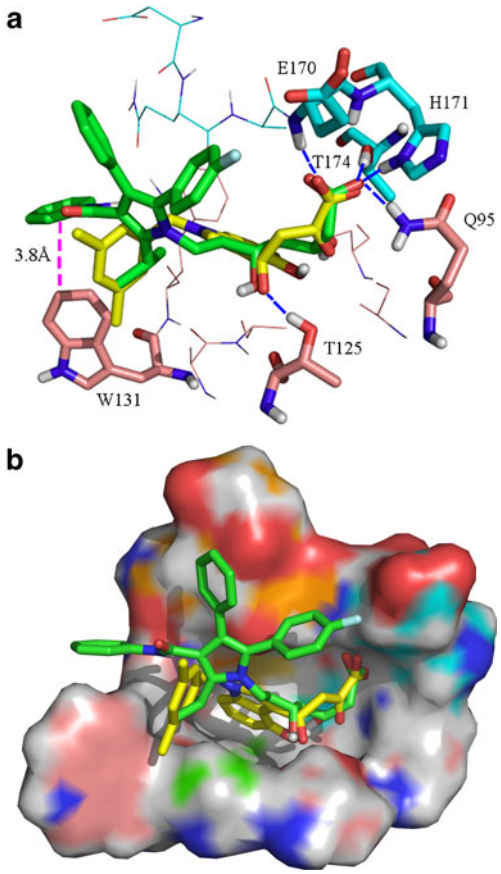

Fig. 7 **a** Docking poses of Atorvastatin (colored green) and CHIBA-3003_5h (colored yellow), key residues were labeled. **b** Atorvastatin and CHIBA-3003_5h are located in binding pocket of IN_CCD dimmer. Pocket's surface is shown for IN. Dash lines represent the non-covalent interactions between the ligand and receptor: blue, H-bonding; pink, π-π interaction

rearrangement of actin cytoskeleton needed for HIV entry and budding. This Rho GTPase inhibition mechanism of statins was related to HMG-CoA reductase inhibition. Another mechanism proposed that statins suppress intercellular cell adhesion molecule 1(ICAM-1)-leukocyte function antigen 1 (LFA-1) interactions that were required for viral entry [34]. Several statins can block the ICAM-1-LFA-1 interaction. It was demonstrated that inhibition of LFA-1 by statins resulted in decreased lymphocyte adhesion to ICAM-1 and impaired T-cell costimulation. This finding indicated that statins might be able to interfere with the immune response. This mechanism was unrelated to HMG-CoA reductase inhibition.

In this study, Atorvastatin can prevent p75 binding upon HIV IN with IC_{50} value of 8.90 μM. Our data indicated a new mechanism in that Atorvastatin inhibits the interaction between p75 and IN and then leads to HIV loads being decreased. This mechanism was unrelated to HMG-CoA reductase inhibition. This study will be useful in helping others plan such experiments.

Conclusions

Using structure-based approach, 26 old drugs were selected and purchased for AlphaScreen assays against p75-IN interaction. Among them, eight old drugs showed IC_{50} values ranged from 6.5 μM to 36.8 μM. The most potent drug Carbidopa can block p75-IN interaction with an IC_{50} value at 6.5 μM, which is on the same inhibitory activity level of some reported potent inhibitors such as CHIBA-3003_5h and compound **6**. These drugs can be a new example of inhibitors targeting protein-protein interaction. In addition, our study suggests that Drug Bank could serve as a good source to accelerate the drug discovery process.

We also explored the binding modes of eight drugs with IN. The key residues for binding are Gln168, Glu170, His171 and Thr174 in A chain, Gln95, Thr125 and Trp131 in B chain. The carboxyl group of all eight drugs formed hydrogen bonding network with the backbone of Glu170, side chain of His171, Thr174 in chain A and Gln95 in chain B. The two most potent drugs create two additional interactions: Carbidopa forms additional hydrogen bonding with Gln168 of chain A and Ala128 of chain B; Atorvastatin forms hydrogen bonding with Thr125 in B chain and π-π stacking with Trp131 in B chain.

In addition, Atorvastatin has already been used in AIDS patients to reduce the amount of cholesterol in infected cells, while multiplication of HIV was also observed to reduce. Our finding suggested that Atorvastatin might target directly to HIV through blocking the p75-IN interaction and provide a clue for further study.

Acknowledgments This work was supported by the Program for New Century Excellent Talents in University (Grant NCET-08-0774), the Innovation Program of Shanghai Municipal Education Commission (Grant 10ZZ41), the National Natural Science Foundation of China (Grants 90813005 and 10979072), the Specialized Research Fund for the Doctoral Program of Higher Education of China (Grant 20090074120012), the 111 Project (Grant B07023), and the Shanghai Committee of Science and Technology (Grant 11DZ2260600). We thank the National Compound Resource Center for providing compounds. The cDNA coding for HIV IN catalytic core domain (IN CCD) (residues 50-212) including the F185K solubilizing-mutation was a gift from Prof. Robert Craigie (National Institutes of Health, Bethesda, MD). The full-length plasmid pCPNat p75 was kindly provided by Prof. Zeger Debyser (Katholieke Universiteit Leuven, Belgium).

References

1. Anthony NJ (2004) HIV-1 integrase: a target for new AIDS chemotherapeutics. Curr Top Med Chem 4:979–990
2. Malet I, Delelis O, Valantin MA, Montes B, Soulie C, Wirden M, Tchertanov L, Peytavin G, Reynes J, Mouscadet JF, Katlama C, Calvez V, Marcelin AG (2008) Mutations associated with failure of raltegravir treatment affect integrase sensitivity to the inhibitor in vitro. Antimicrob Agents Chemother 52:1351–1358. doi:10.1128/Aac.01228-07
3. Van Maele B, Busschots K, Vandekerckhove L, Christ F, Debyser Z (2006) Cellular co-factors of HIV-1 integration. Trends Biochem Sci 31:98–105. doi:10.1016/j.tibs.2005.12.002
4. Llano M, Saenz DT, Meehan A, Wongthida P, Peretz M, Walker WH, Teo WL, Poeschla EM (2006) An essential role for LEDGF/p75 in HIV integration. Science 314:461–464. doi:10.1126/science.1132319
5. Vanegas M, Llano M, Delgado S, Thompson D, Peretz M, Poeschla E (2005) Identification of the LEDGF/p75 HIV-1 integrase-interaction domain and NLS reveals NLS-independent chromatin tethering. J Cell Sci 118:1733–1743. doi:10.1242/jcs.02299
6. Al-Mawsawi LQ, Neamati N (2007) Blocking interactions between HIV-1 integrase and cellular cofactors: an emerging antiretroviral strategy. Trends Pharmacol Sci 28:526–535. doi:10.1016/j.tips.2007.09.005
7. Poeschla EM (2008) Integrase, LEDGF/p75 and HIV replication. Cell Mol Life Sci 65:1403–1424. doi:10.1007/s00018-008-7540-5
8. De Rijck J, Vandekerckhove L, Gijsbers R, Hombrouck A, Hendrix J, Vercammen J, Engelborghs Y, Christ F, Debyser Z (2006) Overexpression of the lens epithelium-derived growth factor/p75 integrase binding domain inhibits human immunodeficiency virus replication. J Virol 80:11498–11509. doi:10.1128/Jvi.00801-06
9. Cherepanov P, Ambrosio ALB, Rahman S, Ellenberger T, Engelman A (2005) Structural basis for the recognition between HIV-1 integrase and transcriptional coactivator p75. Proc Natl Acad Sci USA 102:17308–17313. doi:10.1073/pnas.0506921402
10. Arkin MR, Wells JA (2004) Small-molecule inhibitors of protein-protein interactions: Progressing towards the dream. Nat Rev Drug Discovery 3:301–317. doi:10.1038/Nrd1343
11. Du L, Zhao YX, Chen J, Yang LM, Zheng YT, Tang Y, Shen X, Jiang HL (2008) D77, one benzoic acid derivative, functions as a novel anti-HIV-1 inhibitor targeting the interaction between integrase and cellular LEDGF/p75. Biochem Biophys Res Commun 375:139–144. doi:10.1016/j.bbrc.2008.07.139
12. De Luca L, Barreca ML, Ferro S, Christ F, Iraci N, Gitto R, Monforte AM, Debyser Z, Chimirri A (2009) Pharmacophore-based discovery of small-molecule inhibitors of protein-protein interactions between HIV-1 integrase and cellular cofactor LEDGF/p75. Chem Med Chem 4:1311–1316. doi:10.1002/cmdc.200900070

13. Christ F, Voet A, Marchand A, Nicolet S, Desimmie BA, Marchand D, Bardiot D, Van der Veken NJ, Van Remoortel B, Strelkov SV, De Maeyer M, Chaltin P, Debyser Z (2010) Rational design of small-molecule inhibitors of the LEDGF/p75-integrase interaction and HIV replication. Nat Chem Biol 6:442–448. doi:10.1038/Nchembio.370
14. De Luca L, Ferro S, Gitto R, Barreca ML, Agnello S, Christ F, Debyser Z, Chimirri A (2010) Small molecules targeting the interaction between HIV-1 integrase and LEDGF/p75 cofactor. Bioorg Med Chem 18:7515–7521. doi:10.1016/j.bmc.2010.08.051
15. De Luca L, Ferro S, Morreale F, De Grazia S, Chimirri A (2011) Inhibitors of the Interactions between HIV-1 IN and the Cofactor LEDGF/p75. Chem Med Chem 6:1184–1191. doi:10.1002/cmdc.201100071
16. Prime, version 2.1, Schrödinger, LLC, New York, NY, 2009
17. MacroModel, version 9.7, Schrödinger, LLC, New York, NY, 2009
18. Accelrys Software Inc., Discovery Studio Modeling Environment, Release 2.5, Accelrys, Inc, San Diego, CA, USA, 2004, http://accelrys.com/
19. Fang J, Shen J, Cheng FX, Xu ZJ, Liu GX, Tang Y (2011) Computational insights into ligand selectivity of estrogen receptors from pharmacophore modeling. Mol Inform 30:539–549. doi:10.1002/minf.201000170
20. Kuang GL, Hu GP, Sun XQ, Li WH, Liu GX, Tang Y (2012) In silico investigation of interactions between human cannabinoid receptor-1 and its antagonists. J Mol Model. doi:10.1007/s00894-012-1381-8
21. Hu GP, Kuang GL, Xiao W, Li WH, Liu GX, Tang Y (2012) Performance evaluation of 2D fingerprint and 3D shape similarity methods in virtual screening. J Chem Inf Model. doi:10.1021/ci300030u
22. Jahn A, Hinselmann G, Fechner N, Zell A (2009) Optimal assignment methods for ligand-based virtual screening. J Chem Inf 1:14. doi:10.1186/1758-2946-1-14
23. Jain AN, Nicholls A (2008) Recommendations for evaluation of computational methods. J Comput Aided Mol Des 22:133–139. doi:10.1007/s10822-008-9196-5
24. LigPrep, version 2.3, Schrödinger, LLC, New York, NY, 2009
25. Glide, version 5.5, Schrödinger, LLC, New York, NY, 2009
26. Friesner RA, Banks JL, Murphy RB, Halgren TA, Klicic JJ, Mainz DT, Repasky MP, Knoll EH, Shelley M, Perry JK, Shaw DE, Francis P, Shenkin PS (2004) Glide: a new approach for rapid, accurate docking and scoring. 1. Method and assessment of docking accuracy. J Med Chem 47:1739–1749. doi:10.1021/jm0306430
27. Brooijmans N, Humblet C (2010) Chemical space sampling by different scoring functions and crystal structures. J Comput Aided Mol Des 24:433–447. doi:10.1007/s10822-010-9356-2
28. Jenkins TM, Engelman A, Ghirlando R, Craigie R (1996) A soluble active mutant of HIV-1 integrase: involvement of both the core and carboxyl-terminal domains in multimerization. J Biol Chem 271:7712–7718
29. Hou Y, McGuinness DE, Prongay AJ, Feld B, Ingravallo P, Ogert RA, Lunn CA, Howe JA (2008) Screening for antiviral inhibitors of the HIV integrase - LEDGF/p75 interaction using the AlphaScreen (TM) luminescent proximity assay. J Biomol Screening 13:406–414. doi:10.1177/1087057108317060
30. Zhao Y, Li W, Zeng J, Liu G, Tang Y (2008) Insights into the interactions between HIV-1 integrase and human LEDGF/p75 by molecular dynamics simulation and free energy calculation. Proteins 72:635–645. doi:10.1002/prot.21955
31. Busschots K, Voet A, De Maeyer M, Rain JC, Emiliani S, Benarous R, Desender L, Debyser Z, Christ F (2007) Identification of the LEDGF/p75 binding site in HIV-1 integrase. J Mol Biol 365:1480–1492. doi:10.1016/j.jmb.2006.10.094
32. Penzak SR, Chuck SK (2000) Hyperlipidemia associated with HIV protease inhibitor use: pathophysiology, prevalence, risk factors and treatment. Scand J Infect Dis 32:111–123
33. Del Real G, Jimenez-Baranda S, Mira E, Lacalle RA, Lucas P, Gomez-Mouton C, Alegret M, Pena JM, Rodriguez-Zapata M, Alvarez-Mon M, Martinez-A C, Manes S (2004) Statins inhibit HIV-1 infection by down-regulating Rho activity. J Exp Med 200:541–547. doi:10.1084/Jem.20040061
34. Giguere JF, Tremblay MJ (2004) Statin compounds reduce human immunodeficiency virus type 1 replication by preventing the interaction between virion-associated host intercellular adhesion molecule 1 and its natural cell surface ligand LFA-1. J Virol 78:12062–12065. doi:10.1128/Jvi.78.21.12062-12065.2004